Life Sciences in Space Research 19 (2018) 43–50

Contents lists available at ScienceDirect

Life Sciences in Space Research

journal homepage: www.elsevier.com/locate/lssr

Reduction of geomagnetic field (GMF) to near null magnetic field (NNMF) affects *Arabidopsis thaliana* root mineral nutrition

Ravishankar Narayana[a,1], Judith Fliegmann[b,1], Ivan Paponov[c], Massimo E. Maffei[d,*]

[a] Department of Entomology, Penn State University, W249 Millennium Science Complex, University Park, PA 16802, USA
[b] ZMBP Center for Plant Molecular Biology, University of Tübingen, Tübingen, Germany
[c] Norwegian Institute of Bioeconomy Research, Dept. of Fruit and Vegetables, Ås, Norway
[d] Plant Physiology Unit, Department of Life Sciences and Systems Biology, University of Turin, Turin, Italy

ARTICLE INFO

Keywords:
Arabidopsis thaliana
Helmholtz coils
Gene expression
Ion content
Ion transporters and channels
Near null magnetic field

ABSTRACT

The Earth magnetic field (or geomagnetic field, GMF) is a natural component of our planet and variations of the GMF are perceived by plants with a still uncharacterized magnetoreceptor. The purpose of this work was to assess the effect of near null magnetic field (NNMF, ~40 nT) on *Arabidopsis thaliana* Col0 root ion modulation. A time-course (from 10 min to 96 h) exposure of Arabidopsis to NNMF was compared to GMF and the content of some cations (NH_4^+, K^+, Ca^{2+} and Mg^{2+}) and anions (Cl^-, $SO_4^=$, NO_3^- and $PO_4^=$) was evaluated by capillary electrophoresis. The expression of several cation and anion channel- and transporter-related genes was assessed by gene microarray. A few minutes after exposure to NNMF, Arabidopsis roots responded with a significant change in the content and gene expression of all nutrient ions under study, indicating the presence of a plant magnetoreceptor that responds immediately to MF variations by modulating channels, transporters and genes involved in mineral nutrition. The response of Arabidopsis to reduced MF was a general reduction of plant ion uptake and transport. Our data suggest the importance to understand the nature and function of the plant magnetoreceptor for future space programs involving plant growth in environments with a reduced MF.

1. Introduction

The Earth magnetic field (or geomagnetic field, GMF) is a natural component of the environment and is steadily acting on living systems by influencing many biological processes. The progress and status of research on the effect of magnetic field on plant life have been thoroughly reviewed in the past years (Phirke et al., 1996; Abe et al., 1997; Belyavskaya, 2004; Minorsky, 2007; Teixeira da Silva and Dobranszki, 2015; Teixeira da Silva and Dobranszki, 2016) indicating the presence of a still uncharacterized plant magnetoreceptor. Investigations of the reduction of GMF on biological systems have attracted attention of biologists for several reasons. In space programs, interplanetary navigation will introduce humans, animals and plants in magnetic environments where the magnetic field is at least three orders of magnitude lower than the GMF (i.e., from about 40 μT to near 1 nT) (Maffei, 2014). In fact, the galactic MF induction does not exceed 0.1 nT, in the vicinity of the Sun (0.21 nT), and on the Venus surface (3 nT) (Belov and Bochkarev, 1983). Recent reports indicated that plants respond to “cosmic” or near null magnetic fields (NNMF) with morphological and developmental changes, including the delay in flowering time (Xu et al., 2012; Agliassa et al., 2018a), light-dependent plant processes including germination, leaf movement, stomatal conductance, chlorophyll content and plant vegetative growth (Galland and Pazur, 2005; Maffei, 2014), photoreceptor involvement (Agliassa et al., 2018b) and changes in auxin (Xu et al., 2018) and gibberellin (Xu et al., 2017) levels. Moreover, the delayed transition to flowering caused by NNMF has been correlated to the observed speciation of Angiosperms after geomagnetic field reversals (Maffei, 2014; Occhipinti et al., 2014; Bertea et al., 2015), which does not exclude a hypothetical influence of GMF magnitude and polarity on plant evolution on a geological time-scale.

In both open fields and bioregenerative environments, plants require several essential nutrients of which the macronutrients nitrogen (N) and the minerals potassium (K), calcium (Ca), magnesium (Mg), phosphorous (P) and sulfur (S) are present in plant tissues in relatively large amounts (Marschner, 1995). These nutrients are taken up mainly by roots from the surrounding environment through the activity of specific channels and translocators with multiphasic patterns that

* Corresponding author.
E-mail address: massimo.maffei@unito.it (M.E. Maffei).
[1] These two authors contributed equally to the work.

https://doi.org/10.1016/j.lssr.2018.08.005
Received 3 August 2018; Received in revised form 28 August 2018; Accepted 30 August 2018

depend on varying affinities to their substrates (Maathuis, 2009). For instance, ammonium is mostly taken up in acidic soils, whereas nitrate is the predominant form at higher soil pH (Hachiya and Sakakibara, 2017). Space missions to the Moon, Mars or the large satellites of Jupiter and Saturn to seek new frontiers for human colonization will require regenerative life support systems which necessarily include the production of higher plants, which will necessarily experience an increased radiation and the reduction of gravity and magnetic field (Wolff et al., 2013). Despite the substantial amount of data collected on MIR and the International Space Station (Ferl et al., 2002; Wolff et al., 2013; Kittang et al., 2014), little is known on the effect of NNMF on plant nutrition.

The aim of this work was to assess the effect of GMF reduction on plant mineral nutrition by time-course exposure of Arabidopsis seedlings to NNMF. The results show that reduction of the GMF to NNMF alters both anion and cation uptake by modulating channel and transport activities also at the gene level.

2. Materials and methods

2.1. Plant materials and growth conditions

Arabidopsis thaliana ecotype Columbia-0 (*Col-0*) wild type (WT) seeds were surface sterilized with 70% v/v ethanol for 2 min and then with 5% w/v calcium hypochlorite for 5 min. After 3–4 washes with sterile water, seeds were sown on the surface of sterile agar plates (12 × 12 cm) containing half-strength Murashige and Skoog (MS) medium (Murashige and Skoog, 1962). Plates were sealed with Micropore tape to allow gas exchange and to avoid condensation. Plates were vernalized for 48 h and then exposed vertically under a homogenous and continuous light source at 120 µmol m^{-2} s^{-1} and 21 °C (± 1.5) for 14 h before being kept in the darkness at room temperature for 72 h. Plates were then transferred, in the same laboratory and at the same time, under either NNMF or GMF (controls) (see 2.2) and exposed to 130 µmol m^{-2} s^{-1} white light provided by a high-pressure sodium lamp source (SILVANIA, Grolux 600 W, Belgium) at 21 °C (± 1.5 °C) with a 16/8 light/darkness photoperiod, where germination occurred. All experiments were performed under normal gravity.

2.2. Near null magnetic field (NNMF) generation system and plant exposure

The GMF (or local geomagnetic field) values where typical of the Northern hemisphere at 45°0′59″ N and 7°36′58″ E coordinates. Near-null magnetic field (NNMF) was generated by three orthogonal Helmholtz coils connected to three DC power supplies (model E3642A 50 W, 2.5Adual range: 0–8 V/5A and 0–20 V/2.5A, 50 W, Agilent Technologies, Santa Clara, CA) controlled from a computer via a GPIB connection (Agliassa et al., 2018a). Real-time monitoring of the magnetic field in the plant exposure chamber was achieved with a three-axis magnetic field sensor (model Mag-03, Bartington Instruments, Oxford, U.K.) that was placed at the geometric center of the Helmholtz coils. The output data from the magnetometer were uploaded to a VEE software (Agilent Technologies) to fine-tune the current applied through each of the Helmholtz coil pairs in order to maintain the magnetic field inside the plant growth chamber at NNMF intensity as recently reported (Agliassa et al., 2018a). Defining the vertical axis as "y", the GMF level at the experimental location in our lab was: B_x = 6.39 µT, B_y = 36.08 µT, B_z = 20.40 µT; i.e., a magnetic field strength ($B = [Bx^2 + By^2 + Bz^2]^{½}$) of 41.94 µT; by applying the following voltages Vx = 11.36, Vy = 15.04, Vz = 13.81 (which produced currents I_x = 26 mA, I_y = 188 mA, I_z = 103 mA), the magnetometer values were: B_x = 0.033 µT, By = 0.014 µT, Bz = 0.018 µT with a field strength of 40.11 nT, which is about one thousandth of the GMF strength. Plates containing Arabidopsis seedlings were exposed either to NNMF or to GMF for 10 min, 1 h, 4 h, 24 h, 48 h and 96 h.

2.3. Ion analysis by capillary electrophoresis

For each time point, Arabidopsis roots exposed to either GMF or NNMF were harvested and immediately frozen in liquid nitrogen and the plant material was stored at −80 °C. Cations and anions were extracted from Arabidopsis roots with ultrapure water. Extracts were filtered through 0.2 µm filters and then analyzed by an Agilent 7100 Capillary Electrophoresis System (Agilent Technologies, Santa Clara, CA, US). Ammonium, potassium, calcium and magnesium were analyzed using a bare fused silica capillary with extended light path BF3 (i.d. = 50 µm, I = 56 cm, L = 64.5 cm). Sample injection was at 50 mbar for 5 s with +30 kV voltage and detection wavelength at 310/20 nm. Chloride, sulfate, nitrate and phosphate were analyzed using a bare fused silica capillary with extended light path BF3 (i.d. = 50 µm, I = 72 cm, L = 80.5 cm). Sample injection was at 50 mbar for 4 s with −30 kV voltage and detection at 350/80 nm wavelength. Compounds were identified by using pure standards. The ion content was expressed as mg g^{-1} f wt (except for calcium and magnesium which were expressed in µg g^{-1} f wt).

2.4. RNA extraction from Arabidopsis roots upon time-course exposure to GMF and NNMF

For each time point, 100 mg of frozen Arabidopsis roots exposed to either GMF or NNMF were ground in liquid nitrogen with mortar and pestle. Total RNA was isolated using the Agilent Plant RNA Isolation Mini Kit (Agilent Technologies) and RNase-Free DNase set (Qiagen, Hilden, Germany). Sample quality and quantity was checked by using the RNA 6000 Nano kit and the Agilent 2100 Bioanalyzer (Agilent Technologies) according to manufacturer's instructions. Quantification of RNA was also confirmed spectrophotometrically by using a NanoDrop ND-1000 (Thermo Fisher Scientific, Waltham, MA, US).

2.5. cDNA synthesis and microarray analyses (including MIAME)

Five hundred nanograms of total RNA from each treated sample were separately reverse-transcribed into double-stranded cDNAs by the Moloney murine leukemia virus reverse transcriptase (MMLV-RT) and amplified for 2 h at 40 °C using the Agilent Quick Amp Labelling Kit, two-color (Agilent Technologies). Subsequently, cDNAs were transcribed into antisense cRNA and labeled with either Cy3-CTP or Cy5-CTP fluorescent dyes for 2 h at 40 °C following the manufacturer's protocol. Cyanine-labeled cRNAs were purified using RNeasy Minikit (Qiagen, Hilden, Germany). Purity and dye incorporation were assessed with the NanoDrop ND-1000 UV-VIS Spectrophotometer (Thermo Fisher Scientific) and the Agilent 2100 Bioanalyzer (Agilent Technologies). Then, 825 ng of control Cy3-RNAs and 825 ng of treated Cy5-RNAs were pooled together and hybridized using the Gene Expression Hybridization Kit (Agilent Technologies) onto 4 × 44 K Arabidopsis (v3) Oligo Microarray (Agilent Technologies). The microarray experiment followed a direct 2 × 2 factorial two-color design. For each of the treatment combinations, RNA was extracted and used for hybridization. For each RNA sample, four biological replicates were used. This resulted in 12 two-color arrays, satisfying Minimum Information About a Microarray Experiment (MIAME) requirements (Brazma et al., 2001).

After a 17 h incubation at 65 °C and 10 rpm, microarrays were first washed with Gene Expression Wash buffer 1 for 1 min, then with Gene Expression Wash buffer 2 for 1 min, then with 100% acetonitrile for 30 s, and finally washed in the Stabilization and Drying Solution for 30 s.

Microarrays were scanned with the Agilent Microarray G2505B Scanner with the extended dynamic range (XDR) scan mode to scan the same slide at two different levels and data were extracted and normalized from the resulting images using Agilent Feature Extraction (FE) software (v.9.5.1) (Agilent Technologies).

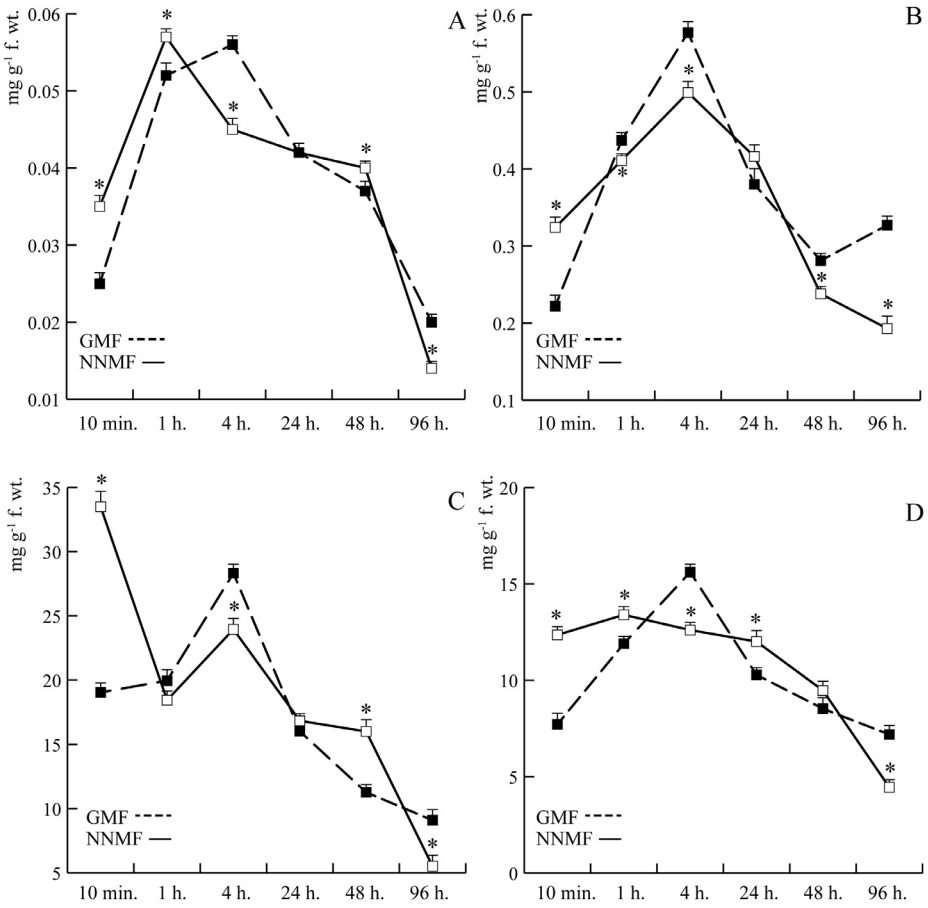

Fig. 1. Cation content of *Arabidopsis thaliana* roots exposed to near null magnetic field (NNMF) with respect to plants growing in geomagnetic field (GMF). **A**. Ammonium; **B**, Potassium; **C**, Calcium; **D**, Magnesium. Data are expressed as the mean value of three replicates. Bars indicate standard deviation. Asterisks indicate significant ($P < 0.05$) differences between GMF and NNMF.

GO enrichment information for the differently expressed probe sets was obtained from The Arabidopsis Information Resource (https://www.arabidopsis.org/index.jsp).

2.6. Validation of microarrays

Validation of the microarray analysis was performed by quantitative real time PCR. First strand cDNA synthesis was accomplished with 1.5 µg total RNA and random primers using the High-Capacity cDNA Reverse Transcription Kit (Applied Biosystems, Foster City, CA, US), according to the manufacturer's instructions. Briefly, the reactions were prepared by adding 10 µl total RNA (1.5 µg), 2 µl of 10X RT Buffer, 0.8 µl of 25X dNTPs mix (100 mM), 2 µl 10X RT random primer, 1 µl of Multiscribe™ Reverse Transcriptase and nuclease-free sterile water up to 20 µl. Then the reaction mixtures were subjected to thermal incubation according to the following conditions; 25 °C for 10 min, 37 °C for 2 h, and 85 °C for 5 s.

All qPCR experiments were performed on a Stratagene Mx3000P Real-Time System (La Jolla, CA, USA) using SYBR green I with ROX as an internal loading standard. The reaction was performed with 25 µl of mixture consisting of 12.5 µl of 2X Maxima™ SYBR Green/ROX qPCR Master Mix (Fermentas International, Inc, Burlington, ON, Canada), 0.5 µl of cDNA and 100 nM primers (Integrated DNA Technologies, Coralville, IA, US). Controls included non-RT controls (using total RNA without reverse transcription to monitor for genomic DNA contamination) and non-template controls (water template). Fluorescence was read following each annealing and extension phase. All runs were followed by a melting curve analysis from 55 to 95 °C. The linear range of template concentration to threshold cycle value (Ct value) was determined by performing a dilution series using cDNA from three independent RNA extractions analyzed in three technical replicates. All primers were designed using Primer 3 software (Rozen, 2000). Primer efficiencies for all primers pairs were calculated using the standard curve method (Pfaffl, 2001). Four different reference genes (cytoplasmic glyceraldehyde-3-phosphate dehydrogenase, (*GAPC2, At1g13440*), ubiquitin specific protease 6 (*UBP6, At1g51710*), β-adaptin (*At4g11380*) and the elongation factor 1B alpha-subunit 2 (*eEF1-Balpha2, At5g19510*) were used to normalize the results of the real time PCR. The best of the four genes was selected using the Normfinder software (Andersen et al., 2004); the most stable gene was the elongation factor 1B alpha-subunit 2.

All amplification plots were analyzed with the MX3000P™ software to obtain Ct values. Relative RNA levels were calibrated and normalized with the level of the elongation factor 1B alpha-subunit 2 mRNA. Results of gene validation for the gene At5g09720 (Mg2 + transporter 8 (MGT8)) performed at 48 h indicates a qPCR value of 1.51 (0.41) with respect to a microarray value of 1.40 (0.18) with no statistical difference ($P > 0.05$).

2.7. Statistical analyses

The data obtained from ion analysis were treated by using Systat 10. Mean value was calculated along with the SD. Paired t test and Bonferroni adjusted probability were used to assess the difference between treatments and the control.

Processing and statistical analysis of the microarray data were done in R using Bioconductor package limma (Smyth, 2005). The raw microarray data are subjected to background subtraction and loess normalized. Agilent control probes were filtered out. The linear models implemented in limma were used for finding differentially expressed genes. Comparisons were made for each of the treatment. Benjamini and Hochberg (BH) multiple testing correction was applied.

Table 1
Time course expression of regulated genes coding for cation transport, channels and exchange in *Arabidopsis thaliana* seedlings exposed to NNMF. Values are expressed as fold change of NNMF values with respect to GMF values (S.D.). See Supplementary Table S1 for all other identified genes.

Gene code	Description	Timing of exposure to NNMF					
		10 m	1 h	4 h	24 h	48 h	96 h
	NH_4^+						
At1g64780	NH_4^+ transporter 1 (AMT1.2)	1.97 (0.34)	−1.29 (0.09)	−1.16 (0.13)	−1.02 (0.14)	2.35 (0.26)	−1.03 (0.21)
At4g28700	NH_4^+ transporter 1 (AMT1.4)	2.66 (0.15)	−1.08 (0.24)	1.18 (0.31)	1.03 (0.18)	2.13 (0.21)	1.08 (0.26)
	K^+						
At2g25600	Inward K^+ channel (AKT6)	1.42 (0.25)	2.16 (0.13)	2.10 (0.27)	2.20 (0.50)	1.46 (0.14)	1.91 (0.27)
At5g46370	outward rectifying K^+ channel (TPK2)	1.35 (0.26)	1.99 (0.22)	2.06 (0.21)	2.41 (0.54)	1.78 (0.17)	1.99 (0.29)
At5g46360	outward rectifying K^+ channel (KCO3)	2.82 (0.16)	2.19 (0.19)	2.63 (0.64)	2.42 (0.49)	1.65 (0.37)	1.80 (0.23)
At1g02510	outward rectifying K^+ channel (TPK4)	1.46 (0.12)	2.42 (0.32)	1.71 (0.45)	1.87 (0.16)	1.47 (0.28)	2.51 (0.26)
	Ca^{2+}						
At1g55720	Ca^{2+} exchanger (CAX6)	2.66 (0.02)	1.41 (0.35)	1.64 (0.30)	1.84 (0.17)	2.26 (0.39)	1.85 (0.25)
At4g29900	Ca^{2+}-transporting ATPase 10 (ACA10)	2.47 (0.60)	−1.13 (0.09)	1.01 (0.08)	−1.02 (0.11)	−1.17 (0.19)	−1.36 (0.15)
At3g57330	Ca^{2+}-transporting ATPase 11 (ACA11)	2.34 (0.14)	−1.26 (0.11)	1.02 (0.03)	−1.08 (0.06)	−1.04 (0.40)	−1.09 (0.10)
At2g22950	Ca^{2+}-transporting ATPase 7 (ACA7)	1.28 (0.24)	1.21 (0.17)	1.63 (0.29)	1.46 (0.05)	2.04 (0.31)	2.04 (0.70)
At3g21180	Ca^{2+}-transporting ATPase 9 (ACA9)	1.59 (0.27)	1.67 (0.42)	1.49 (0.36)	1.4 (0.28)	1.86 (0.30)	2.11 (0.41)
	Mg^{2+}						
At4g28580	Mg^{2+} transporter 5 (MGT5)	1.35 (0.12)	2.11 (0.15)	2.07 (0.30)	2.3 (0.16)	1.43 (0.17)	2.07 (0.21)
At5g09720	Mg^{2+} transporter 8 (MGT8)	2.08 (0.24)	2.13 (0.15)	2.09 (0.30)	2.33 (0.19)	1.40 (0.18)	2.34 (0.40)
At5g09710	Mg^{2+} transporter CorA-like family protein	1.69 (0.52)	−1.12 (0.44)	2.49 (0.35)	−1.53 (0.05)	2.02 (0.35)	−1.94 (0.11)
At2g04305	Mg^{2+} transporter CorA-like protein-related	2.67 (0.63)	1.22 (0.08)	1.22 (0.22)	1.07 (0.14)	1.15 (0.04)	−1.02 (0.13)

3. Results

3.1. Effects of NNMF on root cation content and cation-related gene expression

In general, the root cation content of both GMF and NNMF exposed Arabidopsis varied dramatically along the time-course analyses, particularly after 4 h exposure. Values then normalized their trend with time.

3.1.1. Effects of NNMF on root ammonium content and gene expression

NNMF had a significant effect on the root NH_4^+ content at almost all time of exposure (Fig 1A). Under NNMF, the NH_4^+ content increased at early times (10 min and 1 h), decreased between 4 and 24 h, significantly increased after 48 h and decreased at 96 h, with respect to GMF exposure. The gene ontology (GO) analysis of our microarray data base on genes coding for NH_4^+ transporters identified 6 genes, four of which were not regulated (i.e., fold change $2 > x < -2$) by exposure to NNMF (See Supplementary Table S1), whereas the NH_4^+ transporter *AMT1.2* (At4g13510) and *AMT1.4* (At4g28700) showed an earlier and late upregulation (Table 1).

The upregulation of *AMT1.2* and *AMT1.4* correlated with the early and late increased content of NH_4^+ in Arabidopsis roots exposed to NNMF.

3.1.2. Effects of NNMF on root potassium content and gene expression

Exposure of Arabidopsis to NNMF prompted a very early K^+ increase in root tissues, which was followed by a progressive and significant K^+ reduction, with respect to GMF exposure (Fig. 1B). GO analysis identified 40 genes related to K^+ transport (See Supplementary Table S1), four of which were upregulated by exposure of plants to NNMF (Table 1). In particular, the outward rectifying K^+ channel (*KCO3*, At5g46360), showed a strong upregulation up to 48 h of exposure, whereas the outward rectifying K^+ channels *TPK2* (At5g46370) and *TPK4* (At1g02510) and the inward K^+ channel (*AKT6*) (At2g25600) were upregulated from 1 h exposure to NNMF (Table 1). The increased gene expression of these K^+ outward channels correlated with the decreasing content of K^+ in Arabidopsis roots exposed to NNMF.

3.1.3. Effects of NNMF on root calcium content and gene expression

The Ca^{2+} content of Arabidopsis roots increased consistently after 10 min and 48 h of exposure to NNMF, whereas for the other time points Ca^{2+} values were similar or lower to GMF (Fig. 1C). GO analysis identified 22 genes related to calcium transport (See Supplementary Table S1), five of which showed upregulation in plants exposed to NNMF with respect to GMF (Table 1). In particular, a Ca^{2+} exchanger (*CAX6*, At1g55720) showed a consisted upregulation at 10 min and 48 h (Table 1). Upregulation was also observed for Ca^{2+}-transporting ATPases at 10 min (*ACA10*, At4g29900 and *ACA11*, At3g57330) and 48 h (*ACA7*, At2g22950 and *ACA9*, At3g21180) (Table 1).

The increased calcium content of roots after 10 min and 48 h correlated with the upregulation of both calcium exchanger proteins and the upregulation of some ATP-dependent calcium transporters.

3.1.4. Effects of NNMF on root magnesium content and gene expression

The content of root Mg^{2+} increased in Arabidopsis seedling exposed to NNMF up to 1 h, then it was progressively reduced with time, with the sole exception for 24 h (Fig. 1D). GO analyses identified 14 genes related to Mg^{2+} transport (See Supplementary Table S1), four of which were upregulated at different times under NNMF with respect to GMF (Table 1). Two Mg^{2+} transporters (*MGT5*, At4g28580 and *MGT8*, At5g09720) were upregulated by NNMF at all times, with a reduced upregulation for *MGT5* at 10 min and for both genes at 48 h, whereas a Mg^{2+} transporter *CorA-like related protein* (At2g04305) was downregulated only at 10 min NNMF exposure (Table 1). Mg^{2+} transporter *CorA-like family protein* (At5g09710) showed alternate up- and downregulations after exposure to NNMF (Table 1). A correspondence between Mg^{2+} root content and gene expression was only present at 10 min, 1 h and 24 h for Mg^{2+} transporter CorA-like family proteins.

3.2. Effects of NNMF on root anion content and anion-related gene expression

3.2.1. Effects of NNMF on root chloride content and gene expression

With respect to control seedlings grown in GMF, the Cl^- content significantly ($P < 0.05$) increased in seedlings exposed to NNMF only after 10 min and 48 h exposure (Fig. 2A). GO analysis identified 9 genes related to Cl^- transport (See Supplementary Table S2). Many of these genes were upregulated after 10 min exposure to NNMF such as some Cl^- channels (*CLC-A*, At5g40890; *CLC-B*, At3g27170 and *CLC-G*, At5g33280) and the K^+/Cl^- cotransporter 1 (At1g30450). Two Cl^- channels (*CLC-C*, At5g49890 and *CLC-D*, At5g26240) were upregulated after 48 h, whereas the K^+-Cl^- co-transporter type 1 (*KCC1*,

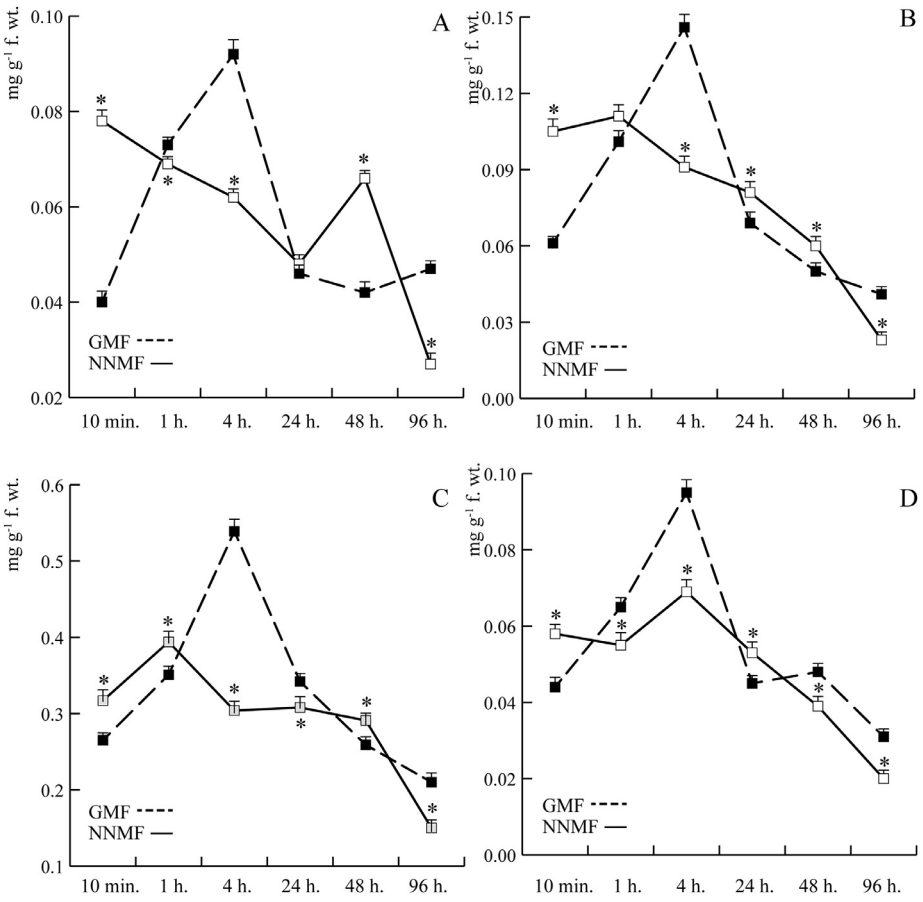

Fig. 2. Anion content of *Arabidopsis thaliana* roots exposed to near null magnetic field (NNMF) with respect to plants growing in geomagnetic field (GMF). **A**. Chloride; **B**, Sulfate; **C**, Nitrate; **D**, Phosphate. Data are expressed as the mean value of three replicates. Bars indicate standard deviation. Asterisks indicate significant ($P < 0.05$) differences between GMF and NNMF.

Table 2
Time course expression of regulated genes coding for anion transport, channels and exchange in *Arabidopsis thaliana* seedlings exposed to NNMF. Values are expressed as fold change of NNMF values with respect to GMF values (S.D.). See also Supplementary Table S2 for all other identified genes.

Gene code	Description	Timing of exposure to NNMF					
		10 m	1 h	4 h	24 h	48 h	96 h
	Cl^-						
At5g40890	Cl^- channel protein (CLC-A)	2.11 (0.37)	−1.10 (0.04)	1.15 (0.04)	1.31 (0.34)	1.02 (0.22)	1.02 (0.11)
At3g27170	Cl^- channel protein (CLC-B)	1.94 (0.14)	−1.24 (0.06)	1.25 (0.20)	1.10 (0.19)	1.50 (0.74)	1.19 (0.17)
At5g49890	Cl^- channel protein (CLC-C)	−1.38 (0.25)	−1.03 (0.01)	1.09 (0.20)	1.11 (0.07)	2.77 (0.77)	−1.03 (0.06)
At5g26240	Cl^- channel protein (CLC-D)	−1.13 (0.06)	−1.03 (0.09)	1.09 (0.10)	1.11 (0.12)	1.90 (0.87)	−1.02 (0.16)
At5g33280	Cl^- channel protein (CLC-G)	2.70 (0.71)	−1.16 (0.11)	−1.12 (0.06)	−1.10 (0.11)	−1.17 (0.16)	−1.11 (0.03)
At3g58370	K^+-Cl^- Co-transporter type 1 (KCC1)	1.57 (0.12)	2.13 (0.14)	1.80 (0.21)	2.33 (0.19)	1.52 (0.11)	1.83 (0.09)
	$SO_4^=$						
At4g08620	$SO_4^=$ transporter (Sultr1;1)	−1.12 (0.16)	2.04 (0.39)	1.59 (0.11)	1.72 (0.36)	−1.07 (0.11)	2.07 (0.36)
At1g22150	$SO_4^=$ transporter (Sultr1;3)	1.25 (0.32)	−1.28 (0.55)	−1.38 (0.23)	−1.33 (0.40)	2.32 (1.38)	1.35 (0.39)
At3g51895	$SO_4^=$ transporter (Sultr3;1)	2.01 (0.65)	1.03 (0.02)	−1.02 (0.25)	1.06 (0.15)	−1.09 (0.07)	−1.04 (0.15)
At3g12520	$SO_4^=$ transporter (Sultr4;2)	−1.02 (0.16)	1.09 (0.14)	1.07 (0.13)	1.10 (0.15)	2.35 (1.27)	−1.01 (0.12)
	NO_3^-						
At1g08100	NO_3^- transporter (ACH2)	−1.04 (0.31)	2.58 (0.46)	2.10 (0.29)	2.58 (0.95)	−1.01 (0.10)	2.24 (0.44)
At1g27080	NO_3^- transporter (NRT1.6)	3.02 (0.41)	1.11 (0.08)	2.01 (0.29)	4.62 (0.31)	1.43 (0.03)	1.53 (0.12)
At5g60770	NO_3^- transporter (NRT2.4)	1.06 (0.10)	2.16 (0.18)	2.15 (0.40)	2.31 (0.24)	1.46 (0.04)	2.36 (0.46)
At3g45060	NO_3^- transporter (NRT2.6)	1.13 (0.04)	1.91 (0.22)	1.14 (0.07)	3.01 (0.49)	1.17 (0.13)	1.84 (0.19)
=	$PO_4^=$						
At5g43360	$PO_4^=$ transporter (PHT1;3)	1.29 (0.29)	2.15 (0.15)	2.11 (0.32)	2.36 (0.40)	1.50 (0.43)	2.37 (0.42)
At5g43340	$PO_4^=$ transporter (PHT1;6)	1.36 (0.18)	2.15 (0.13)	2.09 (0.28)	2.11 (0.15)	1.52 (0.12)	2.39 (0.21)
At1g20860	$PO_4^=$ transporter (PHT1;8)	1.34 (0.28)	2.02 (0.22)	1.76 (0.34)	2.08 (0.17)	1.46 (0.01)	2.08 (0.13)
At1g76430	$PO_4^=$ transporter (PHT1;9)	2.66 (0.65)	1.58 (0.11)	1.34 (0.17)	1.08 (0.35)	1.30 (0.10)	1.83 (0.08)
At5g46110	$PO_4^=$/triose-phosphate translocator (APE2)	2.38 (0.51)	1.14 (0.01)	−1.21 (0.12)	−1.09 (0.06)	−1.02 (0.11)	−1.16 (0.04)

At3g58370) was upregulated after 1 and 24 h (Table 2).

The quantitative analysis of the Cl^- content in Arabidopsis roots correlated with the gene expression of some Cl^- channels, thus indicating a modulation of channel activity dependent on NNMF conditions.

3.2.2. Effects of NNMF on root sulfate content and gene expression

A significant ($P < 0.05$) increase in $SO_4^=$ was found after 10 min, 24 h and 48 h of exposure to NNMF (Fig. 2B). GO analysis identified 11 sulfate transport-related genes (See Supplementary Table S2) of which one (*Sultr3;1*, At3g51895) was upregulated after 10 min NNMF

exposure, two (*Sultr1;3*, At1g22150 and *Sultr4;2*, At3g12520) were upregulated after 48 h and one gene was upregulated after 1 h, 24 h and 96 h (*Sultr1;1*, At4g08620) (Table 2). The upregulation of some $SO_4^=$ transporters is in agreement with the changes in the content of $SO_4^=$ in Arabidopsis seedlings and indicates a differential modulation according to the time of exposure to NNMF.

3.2.3. Effects of NNMF on root nitrate content and gene expression

The content of NO_3^- in Arabidopsis seedling roots varied with time under NNMF with a pattern similar to NH_4^+, with increased contents at 10 min, 1 h and 48 h of exposure (Fig. 2C). Twelve genes involved in NO_3^- transport were identified by GO analysis (See Supplementary Table S2). Three high-affinity genes (*ACH2*, At1g08100; *NRT2.4*, At5g60770 and *NRT2.6*, At3g45060) showed a similar pattern of expression with upregulation at 1 h, 24 h and 96 h, whereas the NO_3^- transporter *NRT1.6* (At1g27080) was upregulated at 10 min, 4 h and 24 h (Table 2). A positive correlation was found between gene expression of NO_3^- transporters and NO_3^- content only at early times of NNMF exposure (10 min and 1 h).

3.2.4. Effects of NNMF on root phosphate content and gene expression

Exposure of Arabidopsis seedlings to NNMF increased the $PO_4^=$ content at 10 min and 24 h, with respect to GMF (Fig. 2D). GO analysis identified 16 genes related to $PO_4^=$ transport (See Supplementary Table S2). The $PO_4^=$ transporter PHT1;9 (At1g76430) and the phosphate/triose-phosphate translocator APE2 (At5g46110) were upregulated at 10 min, whereas the $PO_4^=$ transporters PHT1;3 (At5g43360), PHT1;6 (At5g43340) and PHT1;8 (At1g20860) were upregulated between 1 h and 24 h (Table 2). Even in this case, a positive correlation was found between gene expression of $PO_4^=$ transporters and $PO_4^=$ content only at early and late times of NNMF exposure.

4. Discussion

Reduction of the GMF to NNMF modulates ion content in roots of Arabidopsis seedlings by modulating the gene expression of the major ion transporters and channels. A dramatic change in ion content was found for both cations and anions in GMF and NNMF exposed plants. Daily variations of mineral concentration have already been documented in plants. In tomato, maximal values were reached during the day for NO_3^- and K^+, and during the night for Ca^{2+}, Mg^{2+}, $PO_4^=$, and $SO_4^=$ (Ferrario et al., 1992).

With regards to nitrogen, a close correlation was found between the modulation of NH_4^+ content and the regulation of the plasma membrane localized ammonium transporter *AMT1.2* and *AMT1.4*, members of the AMT subfamily that permeate NH_4^+ via NH_4^+ uniport or NH_3/H^+ cotransport (Ludewig, 2006). Regulation of these genes is usually downregulated by the presence of high amounts of nitrogen and upregulated by nitrogen deficiency (Gazzarrini et al., 1999). We also found a correlation between NNMF-dependent increase of NO_3^- and the upregulation of some high-affinity proton-coupled NO_3^- transporters. In particular, *NRT2.4* plays a role in roots in response to N starvation and is involved in the uptake of NO_3^- at very low external concentration (Kiba et al., 2012), *NRT1.6* is involved in very early stages and is modulated by the external nitrogen supply (Almagro et al., 2008), whereas *NTR2.6* is involved in plant response to pathogen attacks, possibly through the accumulation of reactive oxygen species (ROS) (Dechorgnat et al., 2012). Recently, ROS have been identified as a first biochemical response of plants to NNMF (Bertea et al., 2015; Bhardwaj et al., 2016). Moreover, early gene upregulation occurred for *CLC-A* and *CLC-B*, both members of the voltage-dependent Cl^- channel that also functions as a NO_3^-/H^+ exchanger that serves to accumulate nitrate nutrient in vacuoles (von der Fecht-Bartenbach et al., 2010). Overall, these data indicate that nitrogen transport is affected by NNMF at early times by upregulation of N transport. The increased N content then downregulates the N transporters and generates fluctuations in the N content and gene modulation.

NNMF prompted a strong upregulation of the outward rectifying K^+ channels, with particular reference to *TPK2, KCO3* and *TPK4*, which contain *N*-terminal binding sites for 14-3-3 proteins and putative Ca^{2+} binding EF hands in the cytosolic C-terminal parts, indicating that the channels may be regulated by similar biochemical mechanisms (Voelker et al., 2010). The K^+ content was initially increased by NNMF and then progressively reduced, most probably by the increased activity of outward channels. Interestingly, the early upregulation of high-affinity Ca^{2+}-ATPases [autoinhibited Ca^{2+}-ATPases (*ACA10* and *ACA11*)] and the low-affinity Ca^{2+}/H^+ antiporter (*CAX6*), which are localized in both the plasma membrane and endomembranes (Wang et al., 2016), suggest a Ca^{2+}signaling pathway that may be responsible for K^+ modulation. For instance, expressing *CAX11* in a yeast mutant showed its role of mediating high-affinity K^+ uptake (Zhang et al., 2011). Low MF was found to affect Ca^{2+} homeostasis (Belyavskaya, 2001). The observations of the increase in the $[Ca^{2+}]_{cyt}$ level after exposure to very low MF suggests that Ca^{2+} entry into the cytosol might constitute an early MF sensing mechanism (Belyavskaya, 2001).

Mg^{2+} is important for several biological processes and cellular functions, including DNA replication and posttranscriptional processing and the absorption and transport of Mg^{2+} rely on the transporters (MGT) (Xu et al., 2015). *MGT5* plays a role in transport of Mg^{2+} (Gebert et al., 2009) and its upregulation under NNMF was correlated with increased Mg^{2+} content, particularly at early times.

Along with the above mentioned *CLC-A* and *CLC-B* NO_3^- transporters, the anion channels *CLC-C*, which is involved in Cl^- transport (Jossier et al., 2010), and *CLC-D* and *CLC-G*, which possess a selectivity filter in favor of Cl^- transport (Zifarelli and Pusch, 2009), were also regulated by NNMF. Even in this case, a burst of Cl^- content after 10 min was associated with the upregulation of Cl^- transporters, with particular reference to the CLC class of transporters as well as the K^+–Cl^- cotransporter 1, which symports K^+ and Cl^-, thereby increasing the cellular content of both ions (Kong et al., 2011). in NNMF exposed plants, late reduction of Cl^- content correlated with the reduced expression of most of the genes coding for Cl^- channel proteins.

Another important ion is $SO_4^=$, the major form of inorganic sulfur, an essential element for plants involved in disease resistance, the biosynthesis of sulfur-containing amino acids, and detoxification of ROS (Takahashi et al., 2011). A correlation was found between $SO_4^=$ content and upregulation at early times of *Sultr3;1*, a plastidial $SO_4^=$ transporter (Cao et al., 2013), and after 48 h of *Sultr1;3*, that mediates the inter-organ movement of $SO_4^=$ (Yoshimoto et al., 2003) and *Sultr4;2*, which is upregulated by sulfur limitation (Kataoka et al., 2004). The expression of the $SO_4^=$ transporter *Sultr1;1*, which is localized in the lateral root cap, root hairs, epidermis and cortex of roots (Takahashi et al., 2000), correlated with late variations of $SO_4^=$ content, indicating a major role of this gene in response to NNMF and its possible effects on late $SO_4^=$ reduction. The latter event correlated also with the reduced expression of *Sultr3;1* and *Sultr4;2*.

Phosphorus is a major essential nutrient for plant growth, development and reproduction. Inorganic phosphorus (Pi) is acquired through $PO_4^=$ transporter (PHT) families of which PHT1 are high-affinity Pi transporters mainly located at the plasma membrane (Mudge et al., 2002). A strong upregulation of *PHT1;9*, which acts in the interior of the plant during the root-to-shoot translocation of Pi (Lapis-Gaza et al., 2014), correlated with the increased levels of $PO_4^=$ at early times upon NNMF, and the same pattern was found for *APE2*, a gene that encodes a chloroplast triose phosphate/3-phosphoglycerate translocator that transports triose phosphates derived from the Calvin cycle in the stroma to the cytosol for use in sucrose synthesis and other biosynthetic processes (Flores-Tornero et al., 2017). Late increase of $PO_4^=$ content was associated with the upregulation of *PHT1;3*, a transporter that is induced by interaction with symbiotic fungi (Chen et al., 2007), *PHT1;6*, a plasma membrane-localized proton-coupled Pi transporter that appears also to transport $SO_4^=$, and which is

upregulated by P deficiency (Preuss et al., 2010), and *PHT1;8*, which mediates Pi acquisition under Pi starvation (Remy et al., 2012). The late reduction of $PO_4^=$ correlated with the reduced expression of *APE2*.

5. Conclusions

Reduction of the GMF to NNMF has a significant effect on ion content and ion transport gene expression. A few minutes after exposure to NNMF, plants respond with modulated root content and gene expression of all nutrient ions under study, indicating the presence of a plant magnetoreceptor that responds immediately to MF variations by modulating channels, transporters and genes involved in mineral nutrition. With time, the content of the nutrient ions decreases and is followed by the typical physiological responses of plants exposed to NNMF, including delay of flowering time (Xu et al., 2012; Agliassa et al., 2018a), photoreceptor signaling (Xu et al., 2014; Agliassa et al., 2018b; Vanderstraeten et al., 2018) and seed germination (Soltani et al., 2006). It is interesting to note that the response to NNMF is very rapid, which suggests that some ion channel and transport activity might be dependent on magnetoreception systems not necessarily related to gene expression. Ongoing studies are evaluating the role of ferromagnetic, paramagnetic and diamagnetic metals on plant magnetoreception and the results will be reported soon.

Cosmic exploration will expose plants to reduced MF. The response of the plant magnetoreceptor to reduced MF implies a general reduction of plant ion uptake, transport and, eventually, growth and development. Therefore, it is important to understand the nature and function of the plant magnetoreceptor for future space programs involving plant growth in environments with a reduced MF.

Conflict of interest

The authors declare that there is no conflict of interests.

Acknowledgment

This work was supported by a grant from the University of Turin (local research grants). The authors are grateful to C. Bertea for technical support.

Supplementary materials

Supplementary material associated with this article can be found, in the online version, at doi:10.1016/j.lssr.2018.08.005.

References

Abe, K., Fujii, N., Mogi, I., Motokawa, M., Takahashi, H., 1997. Effect of a high magnetic field on plant. Biol. Sci. Space 11, 240–247.
Agliassa, C., Narayana, R., Bertea, C.M., Rodgers, C.T., Maffei, M.E., 2018a. Reduction of the geomagnetic field delays Arabidopsis thaliana flowering time through down-regulation of flowering-related genes. Bioelectromagnetics 39, 361–374.
Agliassa, C., Narayana, R., Christie, J.M., Maffei, M.E., 2018b. Geomagnetic field impacts on cryptochrome and phytochrome signaling. J. Photochem. Photobiol. B Biol. 185, 32–40.
Almagro, A., Lin, S.H., Tsay, Y.F., 2008. Characterization of the Arabidopsis nitrate transporter nrt1.6 reveals a role of nitrate in early embryo development. Plant Cell 20, 3289–3299.
Andersen, C.L., Jensen, J.L., Orntoft, T.F., 2004. Normalization of real-time quantitative reverse transcription-pcr data: a model-based variance estimation approach to identify genes suited for normalization, applied to bladder and colon cancer data sets. Cancer Res. 64, 5245–5250.
Belov, K.P., Bochkarev, N.G., 1983. Magnetism on the Earth and in Space. Nauka, Moskow.
Belyavskaya, N.A., 2001. Ultrastructure and calcium balance in meristem cells of pea roots exposed to extremely low magnetic fields. Adv. Space Res. 28, 645–650.
Belyavskaya, N.A., 2004. Biological effects due to weak magnetic field on plants. Adv. Space Res 34, 1566–1574.
Bertea, C.M., Narayana, R., Agliassa, C., Rodgers, C.T., Maffei, M.E., 2015. geomagnetic field (Gmf) and plant evolution: investigating the effects of Gmf reversal on *Arabidospis thaliana* development and gene expression. J. Vis. Exp. 105, e53286.
Bhardwaj, J., Anand, A., Pandita, V.K., Nagarajan, S., 2016. Pulsed magnetic field improves seed quality of aged green pea seeds by homeostasis of free radical content. J. Food Sci. Technol. 53, 3969–3977.
Brazma, A., Hingamp, P., Quackenbush, J., Sherlock, G., Spellman, P., Stoeckert, C., Aach, J., Ansorge, W., Ball, C.A., Causton, H.C., Gaasterland, T., Glenisson, P., Holstege, F.C.P., Kim, I.F., Markowitz, V., Matese, J.C., Parkinson, H., Robinson, A., Sarkans, U., Schulze-Kremer, S., Stewart, J., Taylor, R., Vilo, J., Vingron, M., 2001. Minimum information about a microarray experiment (miame) - toward standards for microarray data. Nat. Genet. 29, 365–371.
Cao, M.J., Wang, Z., Wirtz, M., Hell, R., Oliver, D.J., Xiang, C.B., 2013. Sultr3;1 is a chloroplast-localized sulfate transporter in Arabidopsis thaliana. Plant J. 73, 607–616.
Chen, A.Q., Hu, J., Sun, S.B., Xu, G.H., 2007. Conservation and divergence of both phosphate- and mycorrhiza-regulated physiological responses and expression patterns of phosphate transporters in solanaceous species. New Phytol. 173, 817–831.
Dechorgnat, J., Patrit, O., Krapp, A., Fagard, M., Daniel-Vedele, F., 2012. Characterization of the nrt2.6 gene in arabidopsis thaliana: a link with plant response to biotic and abiotic stress. PLoS One 7, 11.
Ferl, R., Wheeler, R., Levine, H.G., Paul, A.L., 2002. Plants in space. Curr. Opin. Plant Biol. 5, 258–263.
Ferrario, S., Agius, I., Morisot, A., 1992. Daily variations of the mineral-composition of xylemic exudates in tomato. J. Plant Nutr. 15, 85–98.
Flores-Tornero, M., Anoman, A.D., Rosa-Tellez, S., Toujani, W., Weber, A.P., Eisenhut, M., Kurz, S., Alseekh, S., Fernie, A.R., Munoz-Bertomeu, J., Ros, R., 2017. Overexpression of the triose phosphate translocator (tpt) complements the abnormal metabolism and development of plastidial glycolytic glyceraldehyde-3-phosphate dehydrogenase mutants. Plant J. 89, 1146–1158.
Galland, P., Pazur, A., 2005. Magnetoreception in plants. J. Plant Res. 118, 371–389.
Gazzarrini, S., Lejay, L., Gojon, A., Ninnemann, O., Frommer, W.B., von Wiren, N., 1999. Three functional transporters for constitutive, diurnally regulated, and starvation-induced uptake of ammonium into arabidopsis roots. Plant Cell 11, 937–947.
Gebert, M., Meschenmoser, K., Svidova, S., Weghuber, J., Schweyen, R., Eifler, K., Lenz, H., Weyand, K., Knoop, V., 2009. A root-expressed magnesium transporter of the mrs2/mgt gene family in arabidopsis thaliana allows for growth in low-mg2+ environments. Plant Cell 21, 4018–4030.
Hachiya, T., Sakakibara, H., 2017. Interactions between nitrate and ammonium in their uptake, allocation, assimilation, and signaling in plants. J. Exp. Bot. 68, 2501–2512.
Jossier, M., Kroniewicz, L., Dalmas, F., Le Thiec, D., Ephritikhine, G., Thomine, S., Barbier-Brygoo, H., Vavasseur, A., Filleur, S., Leonhardt, N., 2010. The arabidopsis vacuolar anion transporter, AtCLCc, is involved in the regulation of stomatal movements and contributes to salt tolerance. Plant J. 64, 563–576.
Kataoka, T., Watanabe-Takahashi, A., Hayashi, N., Ohnishi, M., Mimura, T., Buchner, P., Hawkesford, M.J., Yamaya, T., Takahashi, H., 2004. Vacuolar sulfate transporters are essential determinants controlling internal distribution of sulfate in Arabidopsis. Plant Cell 16, 2693–2704.
Kiba, T., Feria-Bourrellier, A.B., Lafouge, F., Lezhneva, L., Boutet-Mercey, S., Orsel, M., Brehaut, V., Miller, A., Daniel-Vedele, F., Sakakibara, H., Krapp, A., 2012. The Arabidopsis nitrate transporter nrt2.4 plays a double role in roots and shoots of nitrogen-straved plants. Plant Cell 24, 245–258.
Kittang, A.I., Iversen, T.H., Fossum, K.R., Mazars, C., Carnero-Diaz, E., Boucheron-Dubuisson, E., Le Disquet, I., Legue, V., Herranz, R., Pereda-Loth, V., Medina, F.J., 2014. Exploration of plant growth and development using the european modular cultivation system facility on the international space station. Plant Biol. 16, 528–538.
Kong, X.Q., Gao, X.H., Sun, W., An, J., Zhao, Y.X., Zhang, H., 2011. Cloning and functional characterization of a cation-chloride cotransporter gene osccc1. Plant Mol. Biol. 75, 567–578.
Lapis-Gaza, H.R., Jost, R., Finnegan, P.M., 2014. Arabidopsis phosphate transporter1 genes pht1; 8 and pht1;9 are involved in root-to-shoot translocation of orthophosphate. BMC Plant Biol. 14, 19.
Ludewig, U., 2006. Ion transport versus gas conduction: function of AMT/Rh-type proteins. Transfus. Clin. Biol. 13, 111–116.
Maathuis, F.J.M., 2009. Physiological functions of mineral macronutrients. Curr. Opin. Plant Biol. 12, 250–258.
Maffei, M.E., 2014. Magnetic field effects on plant growth, development, and evolution. Front. Plant Sci. 5.
Marschner, H., 1995. Mineral Nutrition in Higher Plants. Academic Press, London.
Minorsky, P.V., 2007. Do geomagnetic variations affect plant function? J. Atmos. Solar–Terr. Phys. 69, 1770–1774.
Mudge, S.R., Rae, A.L., Diatloff, E., Smith, F.W., 2002. Expression analysis suggests novel roles for members of the pht1 family of phosphate transporters in Arabidopsis. Plant J. 31, 341–353.
Murashige, T., Skoog, F., 1962. A revised medium for rapid growth and bioassays with tobacco tissue cultures. Physiol. Plant 15, 473–497.
Occhipinti, A., De Santis, A., Maffei, M.E., 2014. Magnetoreception: an unavoidable step for plant evolution? Trends Plant Sci. 19, 1–4.
Pfaffl, M.W., 2001. A new mathematical model for relative quantification in real-time RT-PCR. Nucleic Acids Res. 29, e45.
Phirke, P.S., Kubde, A.B., Umbarkar, S.P., 1996. The influence of magnetic field on plant growth. Seed Sci. Technol. 24, 375–392.
Preuss, C.P., Huang, C.Y., Gilliham, M., Tyerman, S.D., 2010. Channel-like characteristics of the low-affinity barley phosphate transporter pht1;6 when expressed in xenopus oocytes. Plant Physiol. 152, 1431–1441.
Remy, E., Cabrito, T.R., Batista, R.A., Teixeira, M.C., Sa-Correia, I., Duque, P., 2012. The pht1;9 and pht1;8 transporters mediate inorganic phosphate acquisition by the Arabidopsis thaliana root during phosphorus starvation. New Phytol. 195, 356–371.
Rozen, S., S., H., 2000. Primer3 on the www for general users and for biologist

programmers. In: Krawets, S., M., S.A. (Eds.), Bioinformatics Methods and Protocols. Humana Press, Totowa, pp. 365–386.
Smyth, G.K., 2005. Limma: Linear models for microarray data. In: Gentleman, R., Carey, V., Dudoit, S., Irizarry, R., Huber, W. (Eds.), Bioinformatics and Computational Biology Solutions Using r and Bioconductor. Springer, New York, pp. 397–420.
Soltani, F., Kashi, A., Arghavani, M., 2006. Effect of magnetic field on asparagus officinalis L. seed germination seedling growth. Seed Sci. Technol. 34, 349–353.
Takahashi, H., Kopriva, S., Giordano, M., Saito, K., Hell, R., 2011. Sulfur assimilation in photosynthetic organisms: molecular functions and regulations of transporters and assimilatory enzymes. In: Merchant, S.S., Briggs, W.R., Ort, D. (Eds.), Annual Review of Plant Biology 62. pp. 157–184 vol. 62.
Takahashi, H., Watanabe-Takahashi, A., Smith, F.W., Blake-Kalff, M., Hawkesford, M.J., Saito, K., 2000. The roles of three functional sulphate transporters involved in uptake and translocation of sulphate in Arabidopsis thaliana. Plant J. 23, 171–182.
Teixeira da Silva, J.A., Dobranszki, J., 2015. How do magnetic fields affect plants in vitro? In Vitro Cell Dev. Biol. Plant 51, 233–240.
Teixeira da Silva, J.A., Dobranszki, J., 2016. Magnetic fields: how is plant growth and development impacted? Protoplasma 253, 231–248.
Vanderstraeten, J., Gailly, P., Malkemper, E.P., 2018. Low-light dependence of the magnetic field effect on cryptochromes: Possible relevance to plant ecology. Front. Plant Sci. 9.
Voelker, C., Gomez-Porras, J.L., Becker, D., Hamamoto, S., Uozumi, N., Gambale, F., Mueller-Roeber, B., Czempinski, K., Dreyer, I., 2010. Roles of tandem–pore k plus channels in plants - a puzzle still to be solved. Plant Biol. 12, 56–63.
von der Fecht-Bartenbach, J., Bogner, M., Dynowski, M., Ludewig, U., 2010. Clc-b-mediated no3-/h+ exchange across the tonoplast of arabidopsis vacuoles. Plant Cell Physiol. 51, 960–968.
Wang, F.F., Chen, Z.H., Liu, X.H., Colmer, T.D., Zhou, M.X., Shabala, S., 2016. Tissue-specific root ion profiling reveals essential roles of the CAX and ACA calcium transport systems in response to hypoxia in Arabidopsis. J. Exp. Bot. 67, 3747–3762.
Wolff, S., Coelho, L., Zabrodina, M., Brinckmann, E., Kittang, A., 2013. Plant mineral nutrition, gas exchange and photosynthesis in space: a review. Adv. Space Res. 51, 465–475.
Xu, C., Lv, Y., Chen, C., Zhang, Y., Wei, S., 2014. Blue light-dependent phosphorylations of cryptochromes are affected by magnetic fields in *Arabidopsis*. Adv. Space Res. 53, 1118–1124.
Xu, C., Yu, Y., Zhang, Y., Li, Y., Wei, S., 2017. Gibberellins are involved in effect of near-null magnetic field on Arabidopsis flowering. Bioelectromagnetics 38, 1–10.
Xu, C.X., Yin, X., Lv, Y., Wu, C.Z., Zhang, Y.X., Song, T., 2012. A near-null magnetic field affects cryptochrome-related hypocotyl growth and flowering in Arabidopsis. Adv. Space Res. 49, 834–840.
Xu, C.X., Zhang, Y.X., Yu, Y., Li, Y., Wei, S.F., 2018. Suppression of Arabidopsis flowering by near-null magnetic field is mediated by auxin. Bioelectromagnetics 39, 15–24.
Xu, X.F., Wang, B., Lou, Y., Han, W.J., Lu, J.Y., Li, D.D., Li, L.G., Zhu, J., Yang, Z.N., 2015. Magnesium transporter 5 plays an important role in mg transport for male gametophyte development in arabidopsis. Plant J. 84, 925–936.
Yoshimoto, N., Inoue, E., Saito, K., Yamaya, T., Takahashi, H., 2003. Functional analysis of sulfate transporter sultr1;3, mediating inter-organ movement of sulfate in arabidopsis. Plant Cell Physiol. 44, S173 S173.
Zhang, X.X., Zhang, M., Takano, T., Liu, S.K., 2011. Characterization of an atccx5 gene from arabidopsis thaliana that involves in high-affinity k+ uptake and na+ transport in yeast. Biochem. Biophys. Res. Commun. 414, 96–100.
Zifarelli, G., Pusch, M., 2009. Conversion of the 2 Cl−/1 H+ antiporter CIC-5 in a NO3−/h+ antiporter by a single point mutation. EMBO J. 28, 175–182.